

Cite this: *RSC Adv.*, 2019, **9**, 3140

Surface-attached sulfonamide containing quaternary ammonium antimicrobials for textiles and plastics†

Alexander Caschera, ^a Kamlesh B. Mistry, ^a Joseph Bedard, ^a Evan Ronan, ^a Moiz A. Syed, ^a Aman U. Khan, ^a Alan J. Lough, ^b Gideon Wolfaardt^{ac} and Daniel A. Foucher ^{*a}

With the risks associated with healthcare-associated infections and the rise of antibiotic resistant microorganisms, there is an important need to control the proliferation of these factors in hospitals, retirement homes and other institutions. This work explores the development and application of a novel class of sulfonamide-based quaternary ammonium antimicrobial coatings, anchored to commercially and clinically relevant material surfaces. Synthesized in high yields (60–97%), benzophenone-anchored antimicrobials were spray-coated and UV grafted onto plastic surfaces, while silane-anchored variants were adhered to select textiles *via* dip-coating. Surface modified samples were characterised by advancing contact angle, anionic dye staining, X-ray photoelectron spectroscopy and atomic force microscopy. After verifying coating quality through the above characterization methods, microbiological testing was performed on batch samples in conditions that simulate the natural inoculation of surfaces and objects (solid/air) and water containers (solid/liquid). Using the previously established Large Drop Inoculum (LDI) protocol at solid/air interfaces, all treated samples showed a full reduction (10^5 – 10^7 CFU) of viable *Arthrobacter* sp., *S. aureus*, and *E. coli* after 3 h of contact time. Additional testing of the walls of plastic LDPE vials treated with a UV-cured sulfonamide antimicrobial at a solid/liquid interface using the newly developed Large Reservoir Inoculum (LRI) protocol under static conditions revealed a complete kill ($>10^6$ reduction) of Gram-positive *Arthrobacter* sp., and a partial kill ($>10^4$ reduction) of Gram-negative *E. coli* within 24–48 h of contact.

Received 11th December 2018
 Accepted 13th January 2019

DOI: 10.1039/c8ra10173f

rsc.li/rsc-advances

Introduction

Microbial threat

The proliferation of antibiotic resistance genes within pathogenic microorganisms has become a primary concern of human society in the 21st century. With the gradual emergence of methicillin-resistant *Staphylococcus aureus* (MRSA),^{1,2} vancomycin-resistant *Enterococci* (VRE),^{1,3} and many other multi-drug resistant (MDR) bacterial strains,⁴ there is an ever-increasing threat of contracting an untreatable infection. This threat is further magnified by the concentration of infected patients at hospitals and clinics, where the risk of contracting

a healthcare associated infection (HCAI) during acute care is possible.⁵ Infections acquired at medical centres across North America are responsible for the loss of billions of dollars due to additional hospitalization stays and litigation. According to recent reports published by the Center for Disease Control (CDC), there are an estimated 722 000 nosocomial infections each year in the US, corresponding to 1 infection for every 25 patients admitted. Of those infected, there were 75 000 related deaths during hospitalization, representing a 1 in 10 chance of death from a contracted infection.⁶ At the global level, the World Health Organization (WHO) estimated that 7 of every 100 patients in developed countries and 10 of every 100 patients in developing countries will contract a HCAI. Healthcare costs associated with HCAIs are also astonishing, with WHO estimates placing the financial burden in US dollars at \$8 billion in Europe and \$6.5 billion in the United States.⁵ HCAIs are acquired from multiple routes of exposure including respiratory,⁷ gastrointestinal,^{4,8} cardiovascular,^{9,10} and renal pathways.¹¹ Pathogenic microorganisms suspended in water droplets can cause infections when inhaled or ingested by an individual. These contaminated droplets can transfer pathogens to surfaces such as catheters, gloves and other medical equipment.¹⁰ To combat the emergence and spread of MDR

^aDepartment of Chemistry and Biology, Ryerson University, 350 Victoria Street, Toronto, Ontario, Canada M5B-2K3. E-mail: daniel.foucher@ryerson.ca

^bDepartment of Chemistry, University of Toronto, 80 St. George Street, Toronto, Ontario, Canada M5S 3H6. E-mail: alough@chem.utoronto.ca

^cStellenbosch University Water Institute Secretariat, Faculty of Natural Science, Stellenbosch University, South Africa. E-mail: gmw@sun.ac.za

† Electronic supplementary information (ESI) available: (a) Synthetic details (b) NMR ¹H, ¹³C, ²⁹Si NMR data (c) XPS and ToF-SIMS data, (d) AFM and SP profiles (e) microbiological data. CCDC 1842528 1842536 1842645 1842659. For ESI and crystallographic data in CIF or other electronic format see DOI: 10.1039/c8ra10173f



bacterial strains in institutional settings, several preventative efforts, such as antibiotic stewardship and infection control protocols have been implemented with varying success. Antibiotic stewardship, which relies heavily on compliance by doctors and patients, represents the controlled use of these prescriptions and reduces resistance development by lessening the chance of exposing bacterial cells to sub-lethal drug concentrations.^{12,13} This can also take the form of antibiotic rotation regimens, which regularly swap classes of antibiotics before specific resistance genes can develop within a given microbial population.¹⁴ Infection control programs at hospitals and clinics are used to check the spread of disease between patients and also require strict compliance by patients, visitors and hospital staff.^{1,15} These programs focus on hygienic practices and sterilization techniques to reduce the transfer of microorganisms on contaminated surfaces and individuals. However, adherence to these protocols have yet to prove their efficacy in preventing the proliferation of healthcare associated infectious disease.^{1,16}

To address the rising concerns regarding infection control and contamination from material surfaces, researchers have investigated the application of surface attached antimicrobials to glass,^{17–19} plastic,^{20–22} textiles^{20,21,23} and metals.^{20,24} While the attachment chemistry differs with each surface, the common functional active site design relies on the presence of a long chain (C₁₂–C₂₄) alkyl quaternary ammonium salt which is proposed to impart an adsorbent “phospholipid sponge” effect on cellular membranes through measurable surface charge, thereby damaging cell function and integrity.^{25–27} Long chain QAC materials demonstrate promise as effective microbial resistant coatings when in contact with Gram-positive and Gram-negative bacteria at a solid/air interface,^{18,22,28} and could provide a viable platform for producing self-sterilizing surfaces.²²

To avoid biofilm formation on solid materials under diverse conditions, modifications to QACs through the addition of potent functional moieties have been investigated herein. Dating back to their discovery in 1935, sulfonamide-based antimicrobial drugs represent the initial stages of antibiotic treatment in modern medicine. These compounds evolved into the premier treatment method for infectious disease, such as blood-borne and gastrointestinal infections, but have limitations based on potential toxicity and allergic reaction.²⁹ However, these potent antibiotics may serve effectively as attached sulfa-containing QAC antimicrobials. Even today, new sulfonamide compounds have been developed as sulfa drugs and have shown promising antimicrobial properties against various bacterial and fungal strains.^{30,31}

While there has been significant research effort into preparing non-leaching contact active antimicrobial coatings, there are a limited number of techniques used to assess antimicrobial activity *via* immersive inoculation. More often, the primary goal of biotesting surface-immobilized antimicrobials is to demonstrate that coated materials can prevent microbial proliferation through direct inoculation methods.^{28,32} When immersive solid/liquid interface testing is performed on treated surfaces, it is usually accomplished using the ASTM E2149 shake flask method which simulates submerging an

antimicrobial-treated object into an aqueous body of contaminated liquid.^{28,33} Another method that is used to test for microbial activity at solid/liquid interfaces utilizes a flow cell system, where a nutrient medium is continuously passed through an inoculated flow channel.³⁴ This type of test represents a more dynamic, high shear solid/liquid system where the nutrient medium is replenished during the course of the test and simulates environments similar to catheter tubing or general plumbing. However, limits of this test involve the potential for bacterial species to migrate upstream and establish a biofilm colony in an untreated section of channel, as well as the difficulty of completely treating a full flow system from influent to effluent ports.³⁵

Although there is significant concern with the proliferation of pathogenic microorganisms on dry solid/air surfaces, solid/liquid contact surfaces are also present in many high-risk environments and often provide safe breeding grounds for pathogenic microbes. These surfaces include sinks and drains in hospitals¹⁰ and air cooling towers,⁷ where there is an aqueous medium in sustained contact with a solid container. These microbial niches are areas of concern and can lead to the continuous distribution of microorganisms into new environments,^{3,10} as well as a continuous release of cells as a proliferation mechanism described by Bester *et al.*³⁶ In certain cases, mature biofilms can develop within 24 h and start to release 10⁶ cells per mL.^{36,37} The Liquid Reservoir Inoculum (LRI) method was devised to replicate microbial interactions between solid/liquid interfaces conducted under static, low shear conditions in a controlled environment, as well as provide accurate information regarding antimicrobial activity of constantly wet surfaces.^{38,39} In this work we describe our efforts to prepare and evaluate a series of new shorter chain sulfonamide quaternary ammonium antimicrobials that operate at solid/air interfaces and explore how well these antimicrobial treatments suppress microbial proliferation at solid/liquid surfaces.

Experiments and methods

Materials

All reagents and solvents were obtained from commercial sources and used as received unless indicated otherwise. Stock cotton fabric was sourced from Gildan (cat. G2000-W). Stock plastic polystyrene (PS) (cat. 89106-754) and clear polyvinyl chloride (CPVC) (cat. 82027-788) was sourced from VWR International, Nalgene-brand 5 mL low-density polyethylene (LDPE) vials (cat. 6250-0005) were sourced from ThermoFisher Scientific Inc. and LEXAN-brand polycarbonate (PC) was sourced from Sabic. The trimethoxysilane propyl halide precursor was prepared as previously described by Isquith *et al.*⁴⁰ The benzophenone propyl halide precursor was prepared as previously described by Saettone *et al.*⁴¹ All other experimental details are included in the supplementary section.

Antimicrobial compound characterization

Nuclear magnetic resonance (NMR) experiments were carried out with a 400 MHz Bruker Avance II Spectrometer (Ryerson



University) using deuterated chloroform (CDCl_3) unless otherwise noted. ^1H and ^{13}C spectra were referenced to the residual CHCl_3 (7.26 and 77.0 ppm, respectively) solvent signals, while ^{19}F resonance was referenced against the internal standard CFCl_3 . ^{29}Si NMR was referenced against the internal standard tetramethylsilane (TMS). Peak assignments in the ^1H NMR spectra are given in δ (ppm) and were made with the assistance of 2D COSY spectra, while assignments in the ^{13}C NMR spectra (proton-decoupled) were made with the assistance of 2D HSQC spectra. High resolution mass spectrometry (HRMS) was carried out using electrospray ionization time of flight (ESI-ToF). Melting points were measured in open air using a Fisher Scientific melting point apparatus. A Bruker-Nonius Kappa-CCD diffractometer was used to obtain the X-ray information of the crystal structures of two precursor materials **5** (CCDC 1842645) and **9** (CCDC 1842536) and two active antimicrobials **6a** (CCDC 1842528), and **10** (CCDC 1842659) have been deposited with the Cambridge Crystallographic Data Centre.

Characterization of antimicrobial treated surfaces

Contact angle images of treated and untreated surfaces were taken using a Teli CCD camera equipped with a macro lens attached perpendicularly to the sample surface. Contact angle measurements were performed using OCA15 contact angle software by Data Physics Corporation. X-ray photoelectron spectroscopy (XPS) was performed using a ThermoFisher Scientific K-Alpha, and time-of-flight secondary ion mass spectrometry (ToF-SIMS) was performed using an IonTOF ToF-SIMS IV at the Ontario Centre for the Characterisation of Advanced Materials (OCCAM), located at the University of Toronto. Atomic force microscopy (AFM) using an Asysys nanoIR2 equipped with Contact Mode NIR2 Probes (resonance frequency 13 ± 4 kHz, spring constant $0.07\text{--}0.4 \text{ N m}^{-1}$), and surface profilometry using a KLA-Tencor P16+ Surface Profilometer were also performed at OCCAM. AFM data was processed using Gwyddion 2.50 software.⁴²

Antimicrobial treatment method

Coating of plastic test samples ($6.25 \text{ cm}^2 \pm 1 \text{ cm}^2$ coupons) was performed *via* an ESS AD-LG electrospray apparatus (S/N 20073037, Athens, Georgia) set to spray a 1% (w/v) antimicrobial coating solutions of **1a**–**8a** at 150 kPa. Consistent coating uniformity was achieved by spraying test surfaces for ~ 3 s at an average distance of 45 cm from the spray nozzle. UV curing of benzophenone-anchored QAC **1a**–**8a** coated plastics was performed using a Novacure spot curing system with a mercury-arc discharge lamp at a peak intensity of 10 W, 7 cm from the light guide source. A peak intensity of 0.075 W cm^{-2} monitored over a 60 s curing period, delivered $\sim 5 \text{ J cm}^{-2}$ total dose UVA, as measured using an EIT UV Power Puck 2. Coating solutions of sulfonamide QACs **1b**–**4b** were created by dissolving 1% (w/v) of the desired antimicrobial in an $\text{EtOH} : \text{H}_2\text{O}$ solvent, with the ratio varying between 30 : 70 to 90 : 10 based on the solubility of the test antimicrobial compound. Coating of fabric test samples, ($6.25 \text{ cm}^2 \pm 1 \text{ cm}^2$ swatches of cotton), was performed by dip coating the samples into a coating solution before allowing them to dry at room temperature.

Large droplet inoculum antimicrobial tests

Several clinically relevant bacterial stock cultures were used in these tests. Bacterial test species were grown overnight in 10 mL of 3 g L^{-1} tryptic soy broth (EMD Millipore) at 30°C within a shaking incubator, and cultures were washed twice *via* centrifugation at $9000 \times g$ to replace the growth media with sterile water. *Arthrobacter* sp. (IAI-3), a Gram-positive bacterium originally isolated from indoor laboratory air was inoculated onto all treated and control test surfaces as the model organism for bacterial survival on solid surfaces.³⁹ Lab strains of Gram-negative *Escherichia coli* (DH5 α) and Gram-positive *Staphylococcus aureus* (Ryerson University) were also tested on treated materials. These strains were chosen since they are well characterized and are present in biofilms found within high-risk environments. The large drop inoculum (LDI) method was used to assess the antimicrobial efficacy of the antimicrobial treatment at a solid/air interface and is a modification of the ISO 22196/JIS Z 2801 standard procedure.^{43,44} Triplicate treated samples were inoculated with 100 μL bacterial aliquots of subsequently determined concentration, and survival on the sample was determined by spot plating, described as following. The inoculated droplets were naturally air-dried within a class II, type A2 biosafety cabinet (Model 3440009, Labconco Corp.) to avoid contamination, and surviving cells were enumerated upon drying, typically 3 h after inoculation. Note that the final drying time depends on the evaporation of the inoculum liquid and can be hard to determine on fabric samples due to droplet wicking. Enumeration was performed by rehydrating and vortexing samples in 5 mL of a 0.9% saline retrieval solution, which was then serially diluted and spot-plated onto 3 g L^{-1} tryptic soy agar. Plates were then incubated at 25°C for a period of 5–7 d which allowed for visualization of colony forming units (CFU). At each time point, bacterial survival on the treated samples was compared to survival on triplicate untreated control surfaces of the same material.

Liquid reservoir inoculum antimicrobial tests

Arthrobacter sp. and *E. coli* were grown overnight in 3 g L^{-1} tryptic soy broth at 30°C within a shaking incubator, and cultures were washed twice *via* centrifugation at $9000 \times g$ to replace the growth media with sterile water. The LRI method (Fig. 1) was used to assess the efficacy of the antimicrobial treatment at a solid/liquid interface and is a modification of the ASTM E2149 standard procedure.³³ Triplicate treated 5 mL LDPE tubes containing 2.7 mL of 0.9% sterile saline were inoculated with 300 μL bacterial aliquots of subsequently determined concentration. These tubes were capped and placed onto a VWR orbital shaker (cat. 57018-754) set to 150 rpm for 48 h to prevent sedimentation. At 24 h and 48 h, 100 μL aliquots were removed from the sample, serially diluted and spot-plated onto 3 g L^{-1} tryptic soy agar to enumerate the survival of planktonic cells suspended within the liquid reservoir. After 48 h, sample shaking was suspended, the remaining liquid was replaced with 5 mL sterile saline, and the samples were gently inverted 10 times to rinse any loosely-adhered cells from the tube walls. With the rinse solution discarded, the LDPE tubes



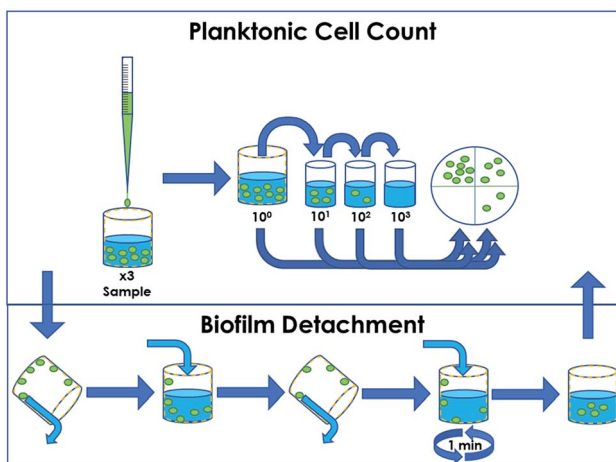


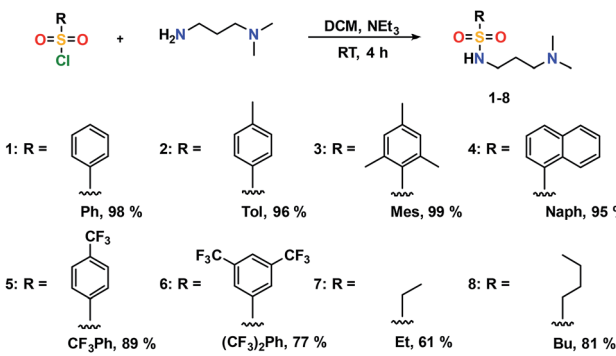
Fig. 1 Simplified schematic representation of the Liquid Reservoir Inoculation (LRI) method.

were then filled with 1 mL of sterile saline and vortexed for 1 min to dislodge any biofilm formed on the tube surface. One 100 μ L aliquot was then removed from each tube, serially diluted and spot-plated to enumerate the survival of biofilm cells attached to the walls of the sample tube. Agar plates were incubated at 25 °C for a period of 5–7 d, which allowed for visualization of CFUs. At each time point, bacterial survival on the treated samples was compared to survival on triplicate untreated control surfaces of the same material.

Results and discussion

Synthesis and characterization of sulfonamide precursors

The addition of 3-(dimethylamino)propylamine to the appropriate sulfonyl chloride in CH_2Cl_2 with NEt_3 for 3 h at room temperature followed by a workup in distilled water produced sulfonamide precursors **1–6** in high yields (Scheme 1). Alkyl sulfonamide precursors **7** and **8** were successfully synthesized in moderate to high yields in the absence of NEt_3 in order to avoid salt formation, while varying the order of addition, with the sulfonyl chloride added to a solution of 3-(dimethylamino) propylamine in CH_2Cl_2 . The non-quaternary ammonium sulfonamide **10** was prepared from the reaction of sulfonamide precursor **9** with 4-hydroxybenzophenone (Scheme 2) and isolated as a yellow crystalline solid.



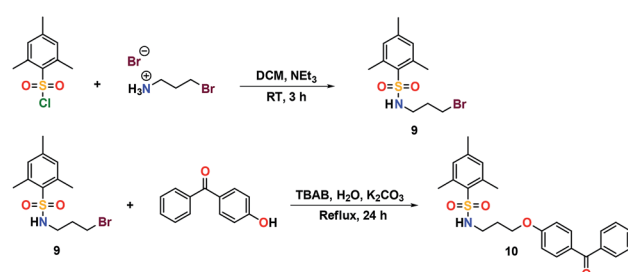
Scheme 1 Preparation of sulfonamides.

Compound **10** was additionally characterized by single crystal X-ray diffraction and an ORTEP representation of the molecule found in the unit cell is displayed in Fig. 2. NMR (^1H and ^{13}C) spectroscopy of all sulfonamide containing compounds, along with HRMS analysis, support their structural identity (ESI).

Synthesis and characterization of sulfaQACs

Further conversion of the sulfonamide precursors to quaternary ammonium salts was achieved using conventional Menshutkin quaternization procedures, which involves heating a mixture of **1–8** and the appropriate haloalkyl silane or benzophenone attachment functionality to reflux in MeCN for extended periods (Scheme 3). Compounds **1a–8a** were recovered as white-coloured crystalline solids, while **1b–4b** were isolated as clear or golden brown-coloured oily gums. These compounds were further purified with successive washes of the crude product with Et_2O (10 mL \times 3).⁴⁵ Compound **6a** was additionally characterized by single crystal X-ray diffraction and an ORTEP representation of the molecule found in the unit cell as displayed in Fig. 3.

For all antimicrobial comparisons, propyl-dimethyl(benzoylphenoxy)octadecylammonium bromide (**11**) was used to provide a baseline antimicrobial activity for alkyl-QAC antimicrobials. This compound was initially detailed by Saettone *et al.*⁴¹ in 1988 for inclusion in sunscreens and investigated by Foucher *et al.* in 2017^{22,46} as antimicrobial coatings on plastic surfaces (Fig. 4).



Scheme 2 Preparation of a UV curable sulfonamide **10**.

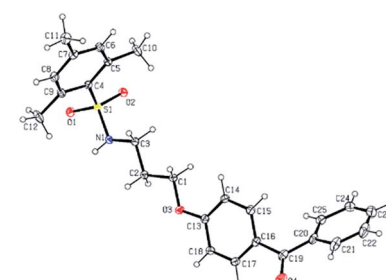
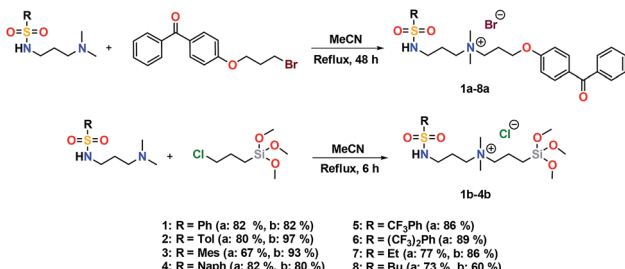


Fig. 2 ORTEP representation of **10** found in the unit cell and selected bond lengths (Å) and bond angles (°): S(1)–O(1) 1.4325(10), S(1)–O(2) 1.4348(9), S(1)–N(1) 1.6203(11), S(1)–C(4) 1.7861(13), N(1)–C(3) 1.4701(17), O(3)–C(1) 1.4337(16), O(3)–C(13) 1.3619(16), O(4)–C(19) 1.2235(18), O(1)–S(1)–O(2) 118.04(6), N(1)–S(1)–C(4) 106.79(6), C(3)–N(1)–S(1) 119.53(9), C(13)–O(3)–C(1) 117.60(10).



Scheme 3 Preparation of sulfaQACs.

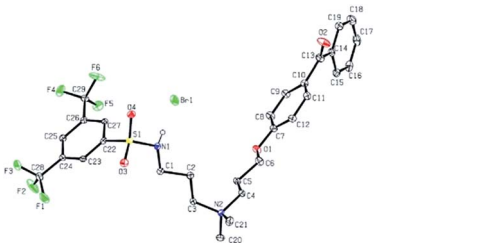


Fig. 3 ORTEP representation of 6a found in the unit cell and selected bond lengths (Å) and bond angles (°): S(1)–O(3) 1.431(2), S(1)–O(4) 1.433(2), N(1)–C(1) 1.469(4), N(2)–C(3) 1.514(3), N(2)–C(4) 1.514(3), N(2)–C(20) 1.499(4), N(2)–C(21) 1.504(4), O(1)–S(1)–O(2) 119.91(13), N(1)–S(1)–C(22) 107.40(13), C(1)–N(1)–S(1) 118.8(2), C(3)–N(2)–C(4) 112.5 (2).

Sulfonamide QAC coating on fabric and polymer samples

Silane-anchored QAC coatings bearing long chain alkyl substituents have been used extensively on porous surfaces for the purpose of protecting against pathogenic infections and to control against odors caused by bacterial metabolites. The rationale behind these efforts is to effectively kill bacterial species before the establishment of a microbial biofilm, thereby preventing the possibility of exposure to contaminated materials. Some of the products treated using these compounds include sporting goods, medical curtains and fabrics, common clothing and protective gear for infection control and odor prevention.⁴⁷ Fabric samples were treated with 1% (w/v) of the active silane-anchored antimicrobial by submerging and agitating cotton swatches within a desired antimicrobial

solution for ~5 min, followed by a 24 h curing period at room temperature. After treatment, samples were exhaustively rinsed with 10 mL aliquots of distilled water and the rinse solution was monitored for antimicrobial leachate with bromophenol blue stain. Once the rinse solution was clear of unadhered antimicrobial, additional samples from each batch were sacrificed for bromophenol blue dye staining to visualize coating quality across the material surface. Commonly, only one rinse step was required to remove excess QAC deposited during the coating process. Coating uniformity was also visualized by submerging test samples in a 400 ppm bromophenol blue dye solution, where treated samples stained blue while leaving uncoated samples unchanged.²² The remaining samples were then used for microbiological evaluation using the LDI procedure with triplicate treated samples compared against controls for antimicrobial activity. Plastic coupons were twice treated with 1% (w/v) of the active benzophenone-anchored antimicrobial to ensure complete coverage. After treatment, samples were rinsed with distilled water, and the rinse solution tested for residual antimicrobial leachate with bromophenol blue stain or by UV-Vis spectroscopy. Once the rinse solution was clear of any unattached antimicrobial, the samples were tested in triplicate under the same conditions as the fabric samples. The mesityl sulfonamide, 3a, was chosen as the primary test candidate among the non-fluorinated sulfaQAC coatings, based on physical characteristics, availability, ease of processing and relatively low cost.

Characterization of antimicrobial coated test surfaces

Several tests were performed to confirm the qualities and characteristics of each antimicrobial coated sample, including dye stain exposure, contact angle, and surface charge measurements. Antimicrobial coated surface quality on polystyrene samples was investigated by advancing contact angle measurements to determine surface wettability (Table 1). SulfaQAC treated materials 1a-4a displayed an advancing contact

Table 1 Advancing contact angle and surface charge measurements of sample materials^a

Sample	Advancing contact angle (°)	Charge density ([N ⁺] nm ⁻²)
Control PS ²²	91.7 ± 1.0	N/A
1a on PS	60.4 ± 4.9	7.3 ± 0.9
2a on PS	51.1 ± 6.5	21.6 ± 6.6
3a on PS	61.0 ± 1.6	23.5 ± 0.7
4a on PS	47.6 ± 0.6	3.5 ± 1.0
5a on PS	73.9 ± 2.1	19.2 ± 3.7
6a on PS	66.7 ± 4.2	15.3 ± 6.8
11 on PS (2 coats) ²²	56.7 ± 1.9	115.0 ± 17.9
C ₁₂ H ₂₅ -N ⁺ (Br) ⁻ on glass ²¹	69	35.7

^a Results collected from this work and ref. 22 were performed in triplicate.

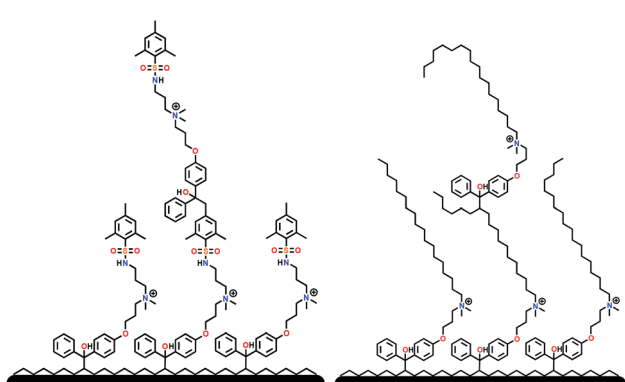


Fig. 4 Schematic representation of surface grafted branching of sulfaQAC 3a (left) and alkylQAC 11 (right).



angle between 47.6° and 61.0° after application of two coats, which is significantly lower than untreated polystyrene (91°), but similar to the long chain QAC **11** (56.7°).²² For the partially-fluorinated sulfaQAC treated materials **5a–6a**, the advancing contact angle was notably higher (73.9° and 66.7°) than non-fluorine containing sulfonamide QACs, but in a similar range to the value reported for the attached benzophenone antimicrobial on glass developed by Locklin *et al.*²⁷ The presence of the quaternary ammonia moiety within the sulfaQACs increase the wettability of these surfaces, while being partially offset by the relative hydrophobicity of the tail moiety.

To compliment the contact angle data, the charge densities of the sulfaQAC antimicrobials were determined indirectly using UV-Vis spectroscopy (Table 1). As outlined by Kugler *et al.*,⁴⁸ this technique involves complexing an anionic dye with the quaternary ammonium cation present on the surface of antimicrobial coatings. After saturating the coating surface in a fluorescein dye solution over a 24 h period and rinsing with distilled water, the bound dye molecules were detached by washing the stained samples in a pH-balanced cationic solution. The solution can then be analysed using a spectrometer to determine dye concentration, which correlates to the number of exposed charges present on a coated sample. Comparing the surface charge and contact angle data values, there appears to be no correlation between the two factors. This could be due to the restricted accessibility of bulky anionic dye molecules to the cationic charges contained within the coated material, or to types of grafted surface structures formed through the coating and curing process. This could also explain the relatively low surface charges of sulfaQACs compared to those found in our previous studies,²² as well as those reported by Locklin²¹ and Murata.⁴⁹ Therefore, the significance of meeting a certain threshold of surface charge as established in previous studies may not be as significant with sulfaQACs, since microbiological testing performed with these materials exhibit similar antimicrobial properties.

Physical properties of **3a** and **6a** treated samples

To further determine the properties and characteristics of sulfaQACs, ToF-SIMS and XPS were performed on a **3a** treated CPVC sample and compared to an untreated control (Table 2). A comparative XPS analysis between the **3a** coated sample and the untreated control showed that there were three significant variations in binding energy peak intensities relating to the

Table 2 Select XPS survey data for control and **3a** treated CPVC samples

Sample	Element	Atomic concentration	Sensitivity factor
Control CPVC	C1s	77.16	1.000
Control CPVC	N1s	0.35	1.800
Control CPVC	S2p	0.93	1.670
3a treated CPVC	C1s	73.17	1.000
3a treated CPVC	N1s	1.84	1.800
3a treated CPVC	S2p	1.24	1.670

carbon, nitrogen and sulfur content (Fig. 5). With relation to the carbon content, there is a significant decrease (3.99%) in carbon present on the coated sample surface compared to the control material, which corresponds to a proportional increase of other elements located within the coating material. There is also an increase in the size of the C1s A (286.6 eV) peak, which indicates the presence of carbon–oxygen ether bond of the benzophenone moiety of **3a**.⁵⁰ Comparisons of the nitrogen content between the two samples showed a notable increase of 1.49% on the treated samples. This increase is seen through the rise of the N1s (402.5 eV) and N1s A (399.9 eV) peaks, which correspond to the presence of cationic nitrogen and carbon–nitrogen bonding within the sample coating.⁵¹ There is also a 0.31% increase in sulfur content found upon the coated samples, similar in significance and scale to the increase of nitrogen content.

ToF-SIMS was also performed on **3a** treated and control CPVC samples (Fig. S7–S11†) to identify and correlate changes in surface structure as related to specific fragments of surface material.⁵² From positive and negative ion fragmentation patterns analyzed from sample materials, the presence of benzoylphenol, tetracarbonyl ammonium and bromide ions were determined to exist on the treated surfaces and are consistent with the composition of **3a**. Through the graphical analysis of ionic fragments found exclusively upon the treated sample, the coating appears to form a relatively irregular patterned surface with $40\text{--}80\text{ }\mu\text{m}$ hemi-spherical structures. Interestingly, there also appears to be small $20\text{ }\mu\text{m}$ diameter structures present when analysing the **3a** coated surface for benzoylphenol, indicative of the benzophenone moiety used to anchor the compound to the CPVC surface (Fig. S11†). To ascertain additional details regarding the coating thickness

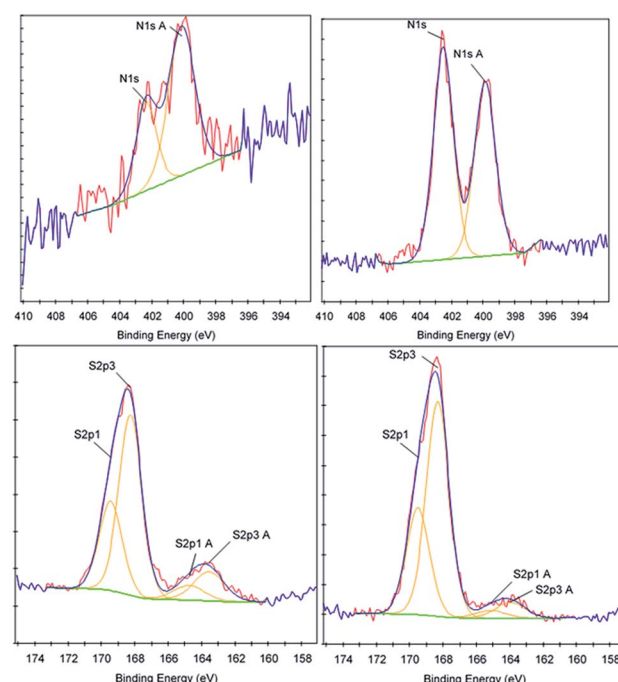
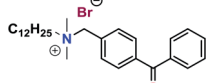


Fig. 5 XPS data corresponding to the nitrogen content (top) and sulfur content (bottom) for control (left) and **3a** treated (right) CPVC samples.



(Table 3) and structure of sulfaQAC treated materials, AFM (Fig. 6 and 7) and SP (Fig. S18–S19†) were performed on **3a** and **6a** treated PC coupons. Samples were prepared by masking a section of the sample surface with an adhesive tape (Scotch 3M®) prior to treatment, followed by a water rinse after tape removal to remove any adhesive residue. The coating thickness of sulfaQACs (**3a**, **6a**) on PC samples (Table 3) is considerably thinner than those found previously for the long-chain alkyl-QAC **11**, which could relate to differences in compound solubility.²² When analyzing the images created from contact-mode AFM scanning on **3a** treated PC plastic, the most strikingly apparent detail involved the roughness of the coated surface when compared to the relatively smooth control material. From the $10 \mu\text{m}^2$ image from Fig. 6, numerous peaks and valleys which have a maximum height difference around $\sim 0.15 \mu\text{m}$ can

Table 3 Thickness measurements of surface attached benzophenone antimicrobials^a

Material	EL (nm)	AFM (nm)	SP (nm)
	42	N/A	N/A
on glass ²¹			
11 treated PS (2 coats) ²²	N/A	366 ± 148	468 ± 159
3a treated PC (2 coats)	N/A	80 ± 29	43 ± 13
6a treated PC (2 coats)	N/A	195 ± 51	125 ± 6

^a Results collected from this work and ref. 22 were taken at three separate sample points.

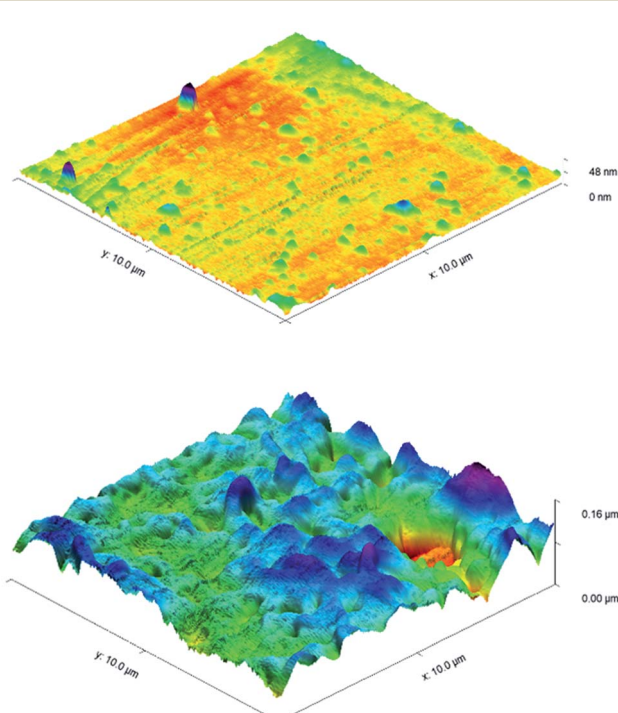


Fig. 6 AFM images of PC control (top) and **3a** treated PC (bottom).

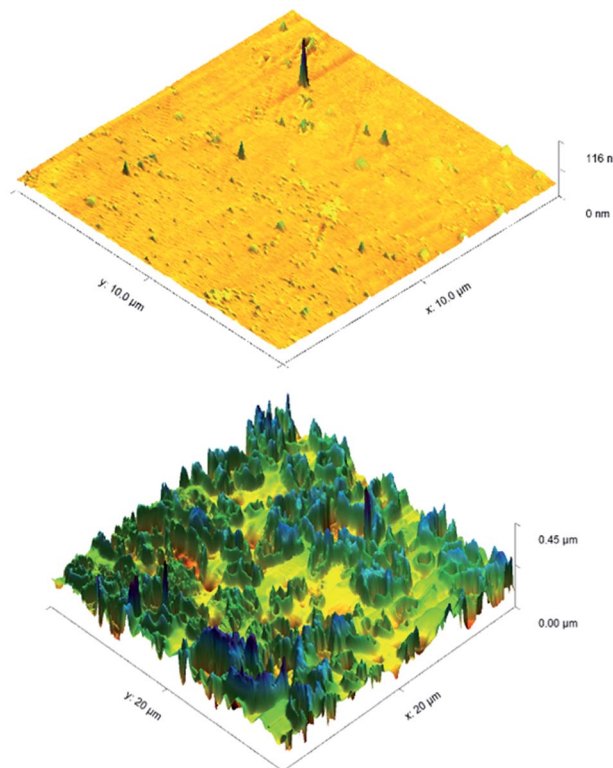


Fig. 7 AFM images of PC control (top) and **6a** treated PC (bottom).

be found scattered across the surface. Collectively, these features provide a root mean square (RMS) roughness measurement of $\sim 20 \text{ nm}$ for a **3a** coated surface, compared to $\sim 4 \text{ nm}$ for the control.

For analysis of **6a** treated PC material, tapping-mode AFM was required to obtain a surface image since there was powerful deflection of the cantilever probe when trying to position the disengaged probe head over the coated surface. The image obtained (Fig. 7) shows a similar change in surface coarseness, providing a RMS roughness value of $\sim 51 \text{ nm}$, but was found to have smoother plateau regions followed by sharp pits and valleys.

Efficacy testing of antimicrobial treatment at solid/air interfaces

The viability and effectiveness of treating non-porous polymer surfaces with benzophenone-anchored sulfaQACs, **1a–4a**, was investigated using the LDI biotesting procedure.^{22,39} Treated samples were tested in triplicate against an uncoated set of controls by inoculating each sample with a subsequently determined microbial cell load and allowing the samples to dry under sterile conditions. The results of these tests (Fig. 8) show promising antimicrobial activity against the Gram-positive representative species, *Arthrobacter* sp. This desiccant tolerant Gram positive bacteria shows good survivability on control samples in comparison to *S. aureus* and *E. coli* (Fig. 13).

A similar LDI experiment with Gram-positive *Arthrobacter* sp. was also investigated for silane-anchored sulfonamide QACs, **1b–4b**, on virgin cotton fabric to determine whether these

antimicrobial treatments remain effective on porous fabric materials (Fig. 9).

This test was also expanded to include fluorinated sulfaQACs, **5a** and **6a**. In comparison to the non-fluorinated **1a–4a**, these more hydrophobic coatings are still effective surface attached antimicrobials as shown through microbiological testing (Fig. 10). This would represent a step towards making tailored, hydrophobic antimicrobial coatings. Interestingly, shorter alkyl-sulfaQACs **7a** and **8a** do not exhibit any significant antimicrobial activity against *Arthrobacter* sp. at solid/air interfaces (Fig. 10).

A complimentary set of Gram-negative trials were also performed on treated plastic and cotton samples using *E. coli* as the test species (Fig. 11 & 12). It was determined that these treated surfaces were similarly effective against the Gram-negative *E. coli* species at solid/air interfaces, suggesting that the presence

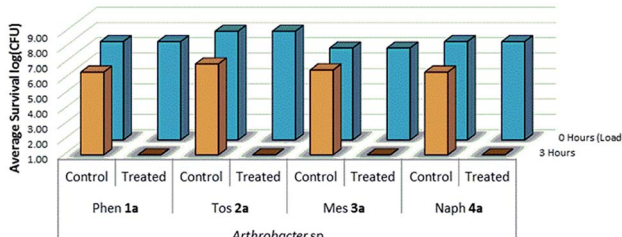


Fig. 8 Survivability of *Arthrobacter* sp. when inoculated onto plastic coupons treated with compounds **1a–4a**, compared against untreated controls. The measurement at 0 h ($>10^7$ CFU for *Arthrobacter* sp.) indicated the initial number of bacterial cells inoculated onto sample material and was determined concurrently to inoculation, while the measurement at 3 h represents a standardized amount of time to allow the inoculum to dry onto a sample surface ($n = 3$).

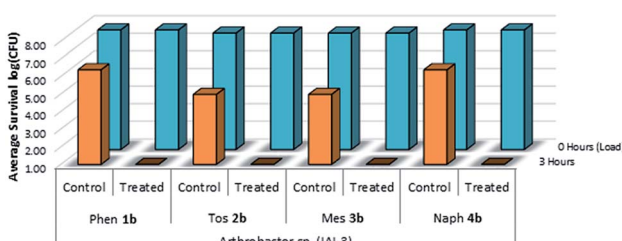


Fig. 9 Survivability of *Arthrobacter* sp. when inoculated onto cotton samples treated with **1b–4b**, compared against untreated cotton controls ($n = 3$).

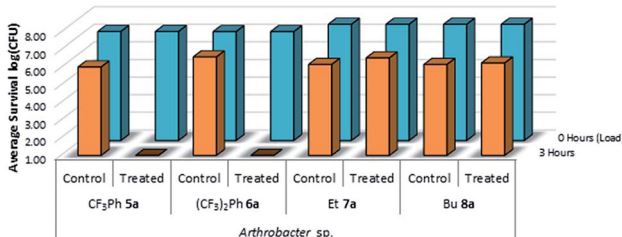


Fig. 10 Survivability of *Arthrobacter* sp. when inoculated onto plastic coupons treated with compounds **5a–8a**, compared against untreated controls ($n = 3$).

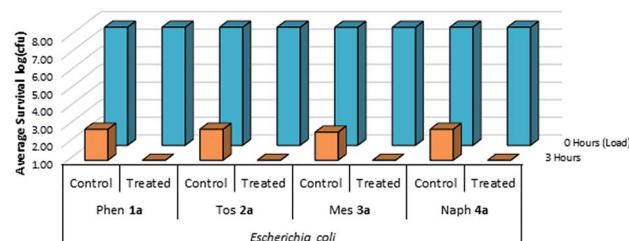


Fig. 11 Survivability of *Escherichia coli* when inoculated onto plastic coupons treated with compounds **1a–4a**, compared against untreated controls ($n = 3$).

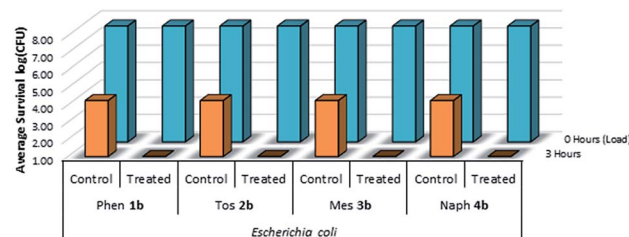


Fig. 12 Survivability of *Escherichia coli* when inoculated onto cotton fabric treated with compounds **1b–4b**, compared against untreated controls ($n = 3$).

of a large exterior peptidoglycan wall does not appear to impact the mechanism of kill during desiccation.

To evaluate the comparative antimicrobial activity of sulfa-QAC treated UV-cured materials, representative Gram-positive and Gram-negative species were chosen for microbiological testing (Fig. 13). Primary tests were performed using an airborne isolate of *Arthrobacter* species, as used previously for LDI testing.²² This Gram-positive bacterial species acts as a model organism for solid/air interface testing, due to its heightened survivability against desiccation at room temperature. Additional tests were performed with Gram-positive *S. aureus* and Gram-negative *E. coli* due to their importance in nosocomial infections, as well as their relation to prevalent antibiotic resistant strains.

To further evaluate how the sulfonamide functionality may impact the antimicrobial activity of QAC coatings, an analogous

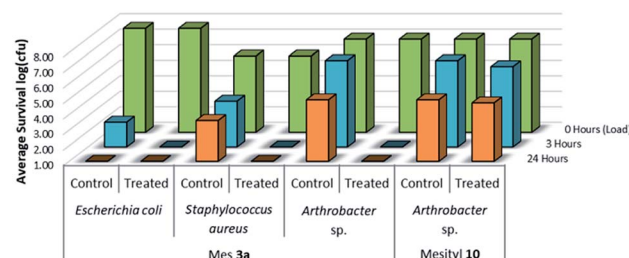


Fig. 13 Survivability of various microorganisms when inoculated onto plastic samples treated with compound **3a** and **10**, compared against untreated plastic controls. The measurement at 0 h ($>10^7$ CFU for *Arthrobacter* sp. and *Escherichia. coli*, $>10^5$ CFU for *Staphylococcus. aureus*) indicated the initial number of bacterial cells inoculated onto sample material and was determined concurrently to inoculation ($n = 3$).

non-quaternary UV-curable sulfonamide **10** (Scheme 3) was tested using the LDI procedure. For this test, PS sample materials were treated with mesityl-based sulfaQAC **3a** or mesityl-based sulfonamide **10** and tested for antimicrobial activity using *Arthrobacter* sp. at 3 h, and at 24 h to determine if there is a weaker antimicrobial effect over time. As shown in Fig. 13, the ammonium-free mesityl sulfonamide coating prepared from **10** exhibited no antimicrobial activity. This would suggest that the sulfonamide functionality of sulfaQACs are independently unable to act as antimicrobial agents without the inclusion of quaternary ammonia.

Efficacy testing of antimicrobial treatment at solid/liquid interfaces

The LRI was designed to complement the LDI method and takes inspiration from industrial standard practices ASTM E2149 (ref. 33) and ISO 22196/JIS Z 2801.^{43,44} The predominant feature of this procedure that differentiates it from the LDI method is that the inoculum remains wet instead of drying out. This prevents desiccation stress from negatively impacting cell survival, but also gives microbial species an avenue to avoid contact with the coated material. To account for this avoidance, the test involved enumerating planktonic cells during the inoculation period and using a harsh rinse procedure to strip and enumerate wall-coated biofilm cells at the end of the test period. The LRI method provides additional advantages in relation to established standard practices (ASTM E2149 and ISO 22196/JIS Z 2801) currently used to test material surfaces for antimicrobial activity. With relation to the ASTM E2149 method, both tests use a liquid inoculum reservoir to inoculate test materials and use mechanical agitation to evenly distribute cells within the test chamber. The advantage brought about by the LRI method involves using the test chamber as the subject of study by applying the microbial treatment directly to the walls of the container, instead of the studied material being placed into the uncoated test chamber. Regarding the ISO 22196/JIS Z 2801 protocol, the sample is kept hydrated by using a cover film to seal and press the inoculum into the test surface. Although this alleviates desiccation stress from the inoculated cells, the cover slip can assist cells in avoiding direct contact with an antimicrobial material by providing a non-antimicrobial surface and a thin liquid gap between the coverslip and the test surface. In contrast, the LRI method avoids untreated surface contact with the liquid inoculum and allows for separate sampling of free-floating planktonic cells and surface-adherent biofilm cells.³²

To determine whether long alkyl chain or sulfonamide QAC antimicrobial coatings can be effective at solid/liquid interfaces, **11** and **3a** were selected as representative candidates for the LRI method. The treated and control LDPE samples containing either **11** or **3a** were tested against Gram-positive *Arthrobacter* sp. and Gram-negative *E. coli*, bacterial species respectively, and showed varying levels of antimicrobial activity.

As shown in Fig. 14, there was no evidence of kill from the long alkyl chain-QAC coating prepared from **11** when compared against control samples except for a slight drop in survivability on both the treated ($>10^3$ CFU) and control ($<10^3$ CFU

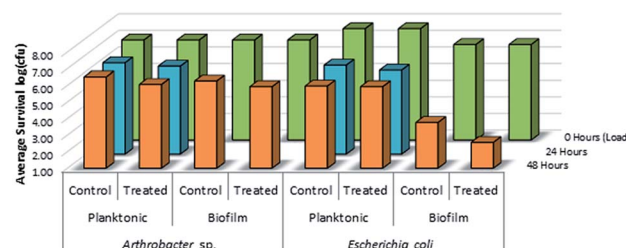


Fig. 14 Survivability of *Arthrobacter* sp. and *Escherichia coli* when inoculated into LDPE vials treated with compound **11**, compared against untreated LDPE controls ($n = 3$).

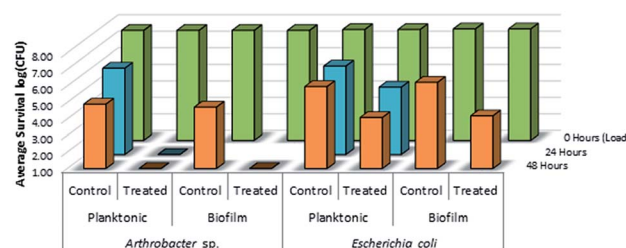


Fig. 15 Survivability of *Arthrobacter* sp. and *Escherichia coli* when inoculated into LDPE vials treated with compound **3a** (mesityl sulfaQAC), compared against untreated LDPE controls ($n = 3$).

remaining) *E. coli* biofilm samples. The drop itself could be related to the lower initial inoculum cell count compared to the other samples, but should not affect the result of comparison between the respective treated and control sets. Compared to the results obtained for **3a** (Fig. 15), the slight drop in *E. coli* biofilm retrievals for **11** is conserved, indicating some slight antimicrobial activity for QAC compounds against Gram-negative species. In contrast, against Gram-positive *Arthrobacter* sp., **3a** showed excellent antimicrobial activity after 24 h and 48 h regarding planktonic cells (Fig. 15). This represents a significant drop in cell survivability compared to control samples at these timepoints ($>10^6$ CFU and $>10^4$ CFU). Against Gram-positive biofilm cells, **3a** can completely reduce the number of viable cells below measurable CFU quantities when compared against untreated controls ($>10^4$ CFU). With Gram-negative *E. coli* cells, **3a** shows reduced antimicrobial activity when compared to the Gram-positive trials. At 24 h ($<10^6$ CFU remaining) and 48 h ($<10^5$ CFU remaining), there is a modest reduction in the number of viable planktonic cells when compared against untreated controls ($>10^6$ CFU and $>10^5$ CFU). This trend of reduced antimicrobial activity is also apparent when comparing treated and control Gram-negative biofilms cells, which shows moderate biocidal activity ($<10^5$ CFU remaining) when compared against untreated controls ($>10^6$ CFU).

Conclusion

Quaternary ammonium antimicrobial treated plastic surfaces are effective at killing pathogenic microorganisms at solid/air interfaces. It has further been demonstrated that significantly

shorter quaternary ammonium compounds bearing sulfonamide functionalities are equally effective at killing bacteria at solid/air interfaces. These sulfaQACs coatings also have unique surface structure properties, ranging from lower surface charges for sulfaQACs ($15.3\text{--}19.5\text{ [N}^+\text{] nm}^{-2}$) when compared to previously studied alkylQACs ($35.7\text{--}115.0\text{ [N}^+\text{] nm}^{-2}$), to changes in surface wettability between non-fluorinated ($47.6\text{--}61.0^\circ$) and fluorinated ($66.7\text{--}73.9^\circ$) QAC coatings. There are also significant changes in surface structure between alkylQAC and sulfaQAC coatings when examined using AFM and SP microscopy techniques. Treatment of plastic surfaces using the mesityl-based sulfaQAC **3a** exhibited promising antimicrobial activity against Gram-negative bacteria (represented by *E. coli*) and excellent antimicrobial activity against Gram-positive bacteria (represented by *Arthrobacter* sp.) when tested at solid/liquid interfaces. By demonstrating solid/liquid antimicrobial efficacy while acting as a non-leaching coating, sulfaQACs shows promise as a novel antimicrobial treatment for constantly wet surfaces, including those found in sinks, drains, commercial air conditioning systems and food processing plants. Additional analysis and biocompatibility studies of sulfaQACs could also lead to their use in medical devices and implants.

Conflicts of interest

There are no conflicts to declare.

Acknowledgements

Funding was provided by Nanosafe Technologies Coating Incorporated, Jupiter Florida, USA, and Viaclean Technologies Philadelphia, PA, USA.

References

- 1 B. J. Hensley and J. R. T. Monson, *Surgery*, 2015, **33**, 528–533.
- 2 C. Makison and J. Swan, *Indoor Built Environ.*, 2006, **15**, 85–91.
- 3 A. Kramer, I. Schwebke and G. Kampf, *BMC Infect. Dis.*, 2006, **6**, 130.
- 4 M. Á. Fernández Fuentes, E. Ortega Morente, H. Abriouel, R. Pérez Pulido and A. Gálvez, *Food Control*, 2014, **37**, 9–14.
- 5 B. Allegranzi, *Report on the Burden of Endemic Health Care-Associated Infection Worldwide Clean Care is Safer Care*, Geneva, Switzerland, 2011.
- 6 S. S. Magill, J. R. Edwards, W. Bamberg, Z. G. Beldavs, G. Dumyati, M. A. Kainer, R. Lynfield, M. Maloney, L. McAllister-Hollob, J. Nadle, S. M. Ray, D. L. Thompson, L. E. Wilson and S. K. Fridkin, *N. Engl. J. Med.*, 2014, **370**, 1198–1208.
- 7 M. K. Ijaz, B. Zargar, K. E. Wright, J. R. Rubino and S. A. Sattar, *Am. J. Infect. Control*, 2016, **44**, S109–S120.
- 8 M. He, F. Miyajima, P. Roberts, L. Ellison, D. J. Pickard, M. J. Martin, T. R. Connor, S. R. Harris, D. Fairley, K. B. Bamford, S. D'Arc, J. Brazier, D. Brown, J. E. Coia, G. Douce, D. Gerding, H. J. Kim, T. H. Koh, H. Kato, M. Senoh, T. Louie, S. Michell, E. Butt, S. J. Peacock, N. M. Brown, T. Riley, G. Songer, M. Wilcox, M. Pirmohamed, E. Kuijper, P. Hawkey, B. W. Wren, G. Dougan, J. Parkhill and T. D. Lawley, *Nat. Genet.*, 2013, **45**, 109–113.
- 9 M. B. Alphonsa, P. T. S. Kumar, G. Praveen, R. Biswas, K. P. Chennazhi and R. Jayakumar, *Pharm. Res.*, 2014, **31**, 1338–1351.
- 10 S. Hota, Z. Hirji, K. Stockton, C. Lemieux, H. Dedier, G. Wolfaardt and M. A. Gardam, *Infect. Control Hosp. Epidemiol.*, 2009, **30**, 25–33.
- 11 P. Singha, J. Locklin and H. Handa, *Acta Biomater.*, 2017, **50**, 20–40.
- 12 G. Cheng, M. Dai, S. Ahmed, H. Hao and X. Wang, *Front. Microbiol.*, 2016, **7**, 1–11.
- 13 S. Harbarth, S. Tuan Soh, C. Horner and M. H. Wilcox, *J. Hosp. Infect.*, 2014, **87**, 194–202.
- 14 P. J. van Duijn and M. J. Bonten, *Trials*, 2014, **15**, 277.
- 15 L. N. G. Duce and J. Fabry, *World Heal. Organ.*, 2002, 1–64.
- 16 M. T. Hawn, C. C. Vick, J. Richman, W. Holman, R. J. Deierhoi, L. A. Graham, W. G. Henderson and K. M. F. Itani, *Ann. Surg.*, 2011, **254**, 494–501.
- 17 I. Banerjee, R. C. Pangule and R. S. Kane, *Adv. Mater.*, 2011, **23**, 690–718.
- 18 F. Siedenbiedel and J. C. Tiller, *Polymers*, 2012, **4**, 46–71.
- 19 G. Becker, Z. Deng, M. Zober, M. Wagner, K. Lienkamp and F. R. Wurm, *Polym. Chem.*, 2018, **9**, 315–326.
- 20 L. M. Porosa, K. B. Mistry, A. Mocella, H. Deng, S. Hamzehi, A. Caschera, A. J. Lough, G. Wolfaardt and D. A. Foucher, *J. Mater. Chem. B*, 2014, **2**, 1509–1520.
- 21 J. Gao, N. E. Huddleston, E. M. White, J. Pant, H. Handa and J. Locklin, *ACS Biomater. Sci. Eng.*, 2016, **2**, 1169–1179.
- 22 L. Porosa, A. Caschera, J. Bedard, A. Mocella, E. Ronan, A. J. Lough, G. Wolfaardt and D. A. Foucher, *ACS Appl. Mater. Interfaces*, 2017, **9**, 27491–27503.
- 23 B. Gottenbos, H. C. Van Der Mei, F. Klatter, P. Nieuwenhuis and H. J. Busscher, *Biomaterials*, 2002, **23**, 1417–1423.
- 24 N. Metoki, L. Liu, E. Beilis, N. Eliaz and D. Mandler, *Langmuir*, 2014, **30**, 6791–6799.
- 25 N. Hadjesfandiari, K. Yu, Y. Mei and J. N. Kizhakkedathu, *J. Mater. Chem. B*, 2014, **2**, 4968–4978.
- 26 Q. Liu, P. Singha, H. Handa and J. Locklin, *Langmuir*, 2017, **33**, 13105–13113.
- 27 J. Gao, E. M. White, Q. Liu and J. Locklin, *ACS Appl. Mater. Interfaces*, 2017, **9**, 7745–7751.
- 28 J. D. Green, T. Fulghum and M. A. Nordhaus, *Biointerphases*, 2011, **6**, MR13–MR28.
- 29 K. C. Nicolaou, J. S. Chen, D. J. Edmonds and A. A. Estrada, *Angew. Chem., Int. Ed. Engl.*, 2009, **48**, 660–719.
- 30 C. Subramanyam, S. Nayab Rasool, D. B. Janakiramudu, S. Rasheed, A. Uday Sankar and C. Naga Raju, *Phosphorus, Sulfur Silicon Relat. Elem.*, 2017, **192**, 845–849.
- 31 H. M. M. Dalloul, K. A. El-Nwairy, A. Z. Shorafa and A. S. Abu Samaha, *Phosphorus, Sulfur Silicon Relat. Elem.*, 2018, **193**, 288–293.



32 J.-B. D. Green, S. Bickner, P. W. Carter, T. Fulghum, M. Luebke, M. A. Nordhaus and S. Strathmann, *Biotechnol. Bioeng.*, 2011, **108**, 231–236.

33 ASTM E2149, 13a: *Standard Test Method for Determining the Antimicrobial Activity of Antimicrobial Agents Under Dynamic Contact Conditions*. 2013, pp. 1–5.

34 O. Kroukamp, R. G. Dumitrache and G. M. Wolfaardt, *Appl. Environ. Microbiol.*, 2010, **76**, 6025–6031.

35 E. Bester, G. M. Wolfaardt, N. B. Aznaveh and J. Greener, *Int. J. Mol. Sci.*, 2013, **14**, 21965–21982.

36 E. Bester, E. A. Edwards and G. M. Wolfaardt, *Can. J. Microbiol.*, 2009, **55**, 1195–1206.

37 E. Bester, O. Kroukamp, M. Hausner, E. A. Edwards and G. M. Wolfaardt, *J. Appl. Microbiol.*, 2011, **110**, 387–398.

38 W. Stone, O. Kroukamp, D. R. Korber, J. McKelvie and G. M. Wolfaardt, *Front. Microbiol.*, 2016, **7**, 1–15.

39 E. Ronan, C. W. Yeung, M. Hausner and G. M. Wolfaardt, *Biofouling*, 2013, **29**, 1087–1096.

40 A. J. Isquith, E. A. Abbott and P. A. Walters, *Appl. Microbiol.*, 1972, **24**, 859–863.

41 M. F. Saettone, C. Alderigi, B. Giannaccini, C. Anselmi, M. G. Rossetti, M. Scotton and R. Cerini, *Int. J. Cosmet. Sci.*, 1988, **10**, 99–109.

42 D. Nečas and P. Klapetek, *Open Phys.*, 2012, **10**, 181–188.

43 ISO 22196:2007, *Plastics — Measurement of Antibacterial Activity on Plastics Surfaces*, 2007, pp. 1–16.

44 JIS Z 2801:2010, *Antibacterial Products - Test for Antibacterial Activity and Efficacy*, 2010, pp. 1–19.

45 D. Foucher, G. Wolfaardt, A. G. Caschera, A. U. Khan, K. Mistry, E. G. Ronan and L. Porosa, Preparation of Sulfonamide-Containing Antimicrobials and Substrate Treating Compositions of Sulfonamide-Containing Antimicrobials, *US Pat.* 20180343870, 2018, pp. 1–85.

46 L. Porosa, A. Mocella, G. Wolfaardt and D. Foucher, UV Cured Benzophenone Terminated Quaternary Ammonium Antimicrobials for Surfaces, *US Pat.* 20150299475, 2015, pp. 1–94.

47 L. Windler, M. Height and B. Nowack, *Environ. Int.*, 2013, **53**, 62–73.

48 R. Kugler, O. Bouloussa and F. Rondelez, *Microbiology*, 2005, **151**, 1341–1348.

49 H. Murata, R. R. Koepsel, K. Matyjaszewski and A. J. Russell, *Biomaterials*, 2007, **28**, 4870–4879.

50 A. V. Shchukarev and D. V. Korolkov, *Cent. Eur. J. Chem.*, 2004, **2**, 347–362.

51 G. Rignanese, A. Pasquarello, J. Charlier, X. Gonze and R. Car, *Phys. Rev. Lett.*, 1997, **79**, 5174–5177.

52 R. E. Goacher, G. Drajeremic and E. R. Master, *Anal. Chem.*, 2011, **83**, 804–812.

